# ALMA Memo 566

# Reflectivity, scattering and emissivity measurements on samples of prospective ALMA reflector panels

Jacob W.M. Baars[1*], Bernard Buzzoni[1], Hans-Peter Gemünd[2] and A. Polsak[3]

June 2001 / December 2006 [1]

1 - European Southern Observatory - Garching, Germany
* now – Max-Planck-Institut für Radioastronomie, Bonn
2 - Max-Planck-Institut für Radioastronomie - Bonn, Germany
3 - ESTEC, Materials and Processes Division - Noordwijk, Netherlands

## 1. Introduction

The frequency coverage and operational conditions of the Atacama Large Millimeter Array (ALMA) put stringent requirements on the reflector surface of the antennas. The major specifications of the reflector can be summarised as follows:

| | | |
|---|---|---|
| 1. overall surface accuracy under all operational conditions | | 25 $\mu$m (20 goal) |
| 2. i ) panel manufacturing error | 8 $\mu$m | |
| ii ) deformation due to temperature differences | 4 $\mu$m | |
| iii) deformation due to gravity and wind forces | 4 $\mu$m | |
| overall panel accuracy in operation | ------- | 12 $\mu$m |
| 3. high reflectivity over frequency range 30 - 1000 GHz | | r > 0.98 |
| 4. capability to observe the Sun without instrumental degradation. | | |

These specifications cause special requirements as to the composition and surface finish of the reflector panels. For instance, a temperature gradient through a panel of about 1 K can easily cause a deformation in excess of the specified 4 $\mu$m. Such a gradient can be expected under the influence of direct sunlight on the panel.

In order to observe the Sun, the solar “heat” must be effectively reflected and also scattered over a wide solid angle in order to avoid an excessive heat load on the cryogenically cooled receiver system in the focal point or on the subreflector and the surrounding structures. Thus it will be necessary to apply some special treatment of a normally “shiny” metal reflector surface to achieve effective wide angle scattering of visible light.

This treatment on the other hand should not cause an unacceptable decrease in the efficiency of reflection of the primary signals of ALMA, the (sub)millimeter waves with frequencies as high as 1 THz. The reflection loss is composed of the so-called “Ruze”-scattering, which results from deviations of the reflector shape from the prescribed geometric form and of “ohmic” losses in the surface. Any small-scale “roughing” of the surface to achieve visible light scattering might contribute to these losses also. The scale and magnitude of this roughness will be in the

[1] This report was begun in 2001, but the sensitivity of the competitive antenna contracts delayed completion and publication to a time where production contracts were in place.

order of one micrometer and thus will not be described well by the Ruze formula. Instead we treat them as increased ohmic loss.

Finally, the surface treatment should also aim at a low absorptance in the visible and low emittance in the near-and middle-infrared wavelengths to avoid excessive heating or cooling of the panel during solar influx or nightly radiation, respectively. These could otherwise cause temperature gradients through the panel of an unacceptable magnitude in view of the specified maximum deformations.

To deal with these issues, different methods and technologies have been proposed by the antenna contractors for the ALMA prototype antennas. Each has provided samples of the proposed reflector surface finishes. We have made a series of measurements on these samples:

i) reflectivity over the frequency range 250 - 1500 GHz, wavelength 0.2 - 1.2 mm,
at MPI for Radio Astronomy, Bonn by Hans-Peter Gemünd,
ii) visible light scattering over 180 degrees angle,
at ESO by Bernard Buzzoni,
iii) emittance and absorptance in the visible and near infrared
at ESTEC, Noordwijk by A. Polsak

## 2. A description of the samples, as provided by the companies

The VertexRSI Corporation, who have produced the "American" prototype antenna, started with machined aluminium samples with grooves machined to different depth and pitch. As we shall see, these were not satisfactory. As a next step samples of sandblasted (un-grooved) aluminium were measured. While these showed acceptable results, the sandblasting procedure had a negative effect on the overall shape accuracy of the full panels. Finally, a good solution was found in chemically etching the machined panels. Several etching procedures were tried. We include here the results of the final panel, as it is being fabricated for the production series of 25 antennas.

For the "European" prototype antenna, the Alcatel-EIE-Consortium (AEC) originally planned to use machined aluminium panels as well. A possible fabricator - Forcier Machine Design (USA) - provided a number of samples. These were machined in a special "cutting pattern" which is proprietary to Forcier. Details have not, to our knowledge, been published.

In addition, ESO had joined a program of ESA/ESTEC with Media Lario of Lecco, Italy, for the development of nickel electroformed panels. These panels are replicated by deposition of a nickel skin on a steel mold which is accurately machined in the prescribed shape. Light sandblasting of the mold surface provides a slightly rough surface at the micrometer level, which was expected to be advantageous for the scattering of the visible light. An advantage here is that the sandblasting takes place on a massive mold instead of the thin panel surface, as was the case with the Vertex method. Eventually, AEC decided to use panels in the Media Lario (ML) technology for the prototype antenna.

A number of samples with different surface finish, including sandblasting, were provided by Media Lario. Because the thermal characteristics of the nickel surface were unsatisfactory for our purpose, different coatings were tried. Thin coatings (200 nm) of both aluminium and rhodium were applied. The final decision was in favour of a rhodium coating. The prototype antenna of AEC was delivered with such panels and measurements on this are reported here.

Panels of this type are also fabricated by Media Lario for the 25 production antennas, delivered by the Alenia-Alcatel-EIE-MT (AEM) consortium.

The samples and their major characteristics are presented in Table 1.

**Table 1: The set of tested samples**

| Company | Code | Material | Surface finish | Details |
|---|---|---|---|---|
| Vertex | V1 | Aluminium | grooves | 3° angle – 250 $\mu$m pitch |
| „ | V2 | „ | grooves | 6° – 250 $\mu$m |
| „ | V3 | „ | grooves | |
| „ | VS1 | „ | sandblasted | 1 bar, long duration |
| „ | VS2 | „ | sandblasted | polished, 1 bar long |
| „ | VS3 | „ | sandblasted | 2 bar, short duration |
| „ | VM1 | „ | fine-machined | clear |
| „ | VM2 | „ | machined | thin white paint layer |
| „ | VM3 | „ | machined | chemically etched, 15 minutes |
| „ | VM4 | „ | machined | chemically etched, 30 min. |
| „ | VM-final | „ | machined | chemically etched |
| Forcier | F1 | Aluminium | grooves | 10 $\mu$m deep - 150 $\mu$m pitch |
| „ | F2 | „ | grooves | 15 $\mu$m - 150 $\mu$m |
| „ | F3 | „ | grooves | 10 $\mu$m - 200 $\mu$m |
| „ | F4 | „ | grooves | 15 $\mu$m - 200 $\mu$m |
| Media Lario | ML1 | Aluminium | "clear" | |
| „ | ML2 | Nickel | sandblasted | |
| „ | ML3 | Nickel | "clear" | |
| „ | ML4 | „ | sandblasted | |
| „ | ML5 | „ | sandblasted | Alu coating |
| „ | ML6 | „ | sandblasted | Alu coating |
| „ | ML7 | Aluminium | "clear" | |
| „ | ML8 | Nickel | sandblasted | Alu coating |
| „ | ML9 | „ | sandblasted | |
| „ | ML10 | „ | "clear" | |
| „ | ML-final | Nickel | | Rhodium coating, 200 nm |

Note that there is no significant difference between similarly described samples in the Media Lario set. The idea was to obtain some "statistics" on a small sample. The ML samples were obtained by an electroforming process on a mandrel. All samples are flat rectangular discs and have a size of 50 x 50 mm, prescribed by the geometry of the measuring instrument at MPIfR.

In the following sections we summarise the results of the different measurements performed. These are presented in tabular form in Table 2 and by graphs, where appropriate. Text input, in addition to the measurement results, has been provided in the following way:

Section 3: reflectivity at wavelengths from about 1.5 mm to 0.2 mm by Gemünd,
Section 4: scattering distribution of visible light over 180 degrees by Buzzoni,
Section 5: thermo-optical properties in the visible-near infrared by Polsak.

A short discussion of the results is presented in the last section (6), written by Baars. It is hoped that this compilation might be of use to others who are developing submillimeter and far-infrared reflectors.

## 3. Measurement of reflectivity at wavelengths from 0.2 to 1.5 mm (Gemünd)

### 3.1. The measurement set-up

The measurements were performed with a commercial Fourier Transform Spectrometer (FTS) (BOMEM DA3.26) of the Division for Submillimeter Technology at the MPIfR in Bonn. The spectrometer has been modified in two aspects:

i) the reflection-stage is non-commercial and offers a well defined plane for the sample holder and hence for the surface under investigation. The stage allows to work with several, fixed, angles of incidence. For our investigation an angle of 11.25° has been chosen. This value is the smallest possible close to normal incidence. Due to the necessary separation between illuminating and reflected beam, the reflection under vertical incidence can not be measured.

ii) the detector is an MPIfR-developed bolometer system. By carefully combining suitable bolometers and filters it has been possible to achieve a sufficiently high signal to noise ratio over a frequency region from 0.3 - 1.5 THz (wave numbers 10 - 50 $cm^{-1}$, wavelength 0.2 - 1 mm).

FTS-measurements of optical properties close to a value of one are delicate and this holds especially in case of reflection, as any reflective reference is known with limited accuracy (typically a few tenths to one percent). Here all spectra are calibrated against the same reference: a 100 nm thick gold-film, evaporated onto an optically polished metal mirror.

At the beginning, it was not clear whether the samples could have spectral features on a small frequency scale, so the first measurements started with a relatively high spectral resolution of 0.1 $cm^{-1}$, which is equivalent with long integration times. After a few runs it became clear that measurements in general would be afflicted by the following environmental effects:

a) there were heavy vibrations in the building, originating from directly adjacent construction activity,

b) there were temperature drifts in the air-conditioning system of the laboratory. Later on, during the last series of measurements, these sources of interference were negligible. However, now measurements were often afflicted by:

c) temperature switching in the water line providing cooling of the spectrometer source.

Ad a): vibrations cause spurious spikes in the spectrum and normally can be shifted, and thereby identified, by varying the scan speed. Unfortunately, noise form construction activity is never sufficiently homogeneous and stable to enable a clear distinction between microphony and a real spectral feature. Consequently some uncertainty in the single measurement remains.

Ad b): as long as they are moderate, temperature changes should not influence the spectrometer much, although there might be some effect in the spectrum close to the ends of the frequency window, where even the reference signal is small. Unfortunately, the observed changes in the room temperature were not at all moderate. Thus this influence increased with a longer measurement time for a single spectrum, i.e. with higher spectral resolution. As a result, repeated reference spectra could miss the 100%-level in the form of a steady incline or decline over the entire spectral range.

Ad c): in contrast to this, thermal switching in the cooling water (up to 2°C within one minute) is a severe cause of variation in the emissivity of the source. Hence it is not surprising that this can be seen directly as a pseudo-oscillation in the normally smooth spectrum. As it turned out, this temperature switching in the water-line was observed here for the first time and it took

considerable time to localise the problem. We found that the air-conditioning and the cold-water-line are fed by the same cooling system via a controller which did not work properly.

As mentioned, the reflectivity of the reference normally is known with an accuracy of about one percent. Hence the measured reflectance of samples close to one will exhibit an accuracy of the same order. This holds for normal circumstances, whereas the problematic measuring situation for these samples was rather more unfavourable. Nevertheless, an attempt was made to gather reliable data as close as possible to the limits of photometric accuracy. This was done by comparing several spectral measurements of the same sample under varying circumstances, i.e. two different bolometer detector systems, three scan speeds and two resolutions of 0.1 and 0.5 $cm^{-1}$. As no significant differences could be observed, highly resolved spectra were smoothed and at the end all spectra were taken together to form an arithmetic average. This results in a spectral resolution of 0.5 $cm^{-1}$ or better for the average spectrum of the first series of measurements. For the radio astronomer, more used to frequency than wave-number, a resolution of 0.1 $cm^{-1}$ is equivalent to a spectral resolution of 3 GHz.

Because no high-frequency spectral details were to be expected, the resolution of the second series of measurements was set at 0.2 $cm^{-1}$ (6 GHz). In the analysis these spectra were also averaged to the same spectral resolution of 0.5 $cm^{-1}$ (15 GHz) as those of the first series. The photometric accuracy of the average spectrum is derived from successive reference spectra and is estimated to be $\Delta R/R = \pm 1\%$ for the first series and $\pm 2.5\%$ during the second series. It is interesting to note that in both cases the absolute temperature changes were more or less equal ($\Delta T = 5^{\circ}C$), so the loss in accuracy is to be attributed to the fast temporal gradients in the temperature of the cooling water.

### 3.2. Results and discussion

We show the results of the measurements in two forms. Most samples, in particular those with the sandblasted surface finish, show an essentially constant reflectivity within the measurement accuracy over the entire wavelength band from 0.2 to 1.0 mm. The reflectivity values for all samples are given in Table 2 for the frequencies 300, 600 and 1000 GHz. For most of these a slight decrease in reflectivity with increasing frequency is visible in the spectrograms. The deviation from the measured reference spectrum is of the order of one percent, comparable to the measurement accuracy. Thus it can be stated that the submillimeter wavelength reflectivity of all samples is fully acceptable with the obvious exception of the painted Vertex sample. There is some indication that the finely machined Forcier panels begin to show decreasing reflection above 1 Thz. A similar feature is visible in the spectrum of the laser annealed sample (VM5). The spectra of the final material choices are shown in Figures 1 and 2.

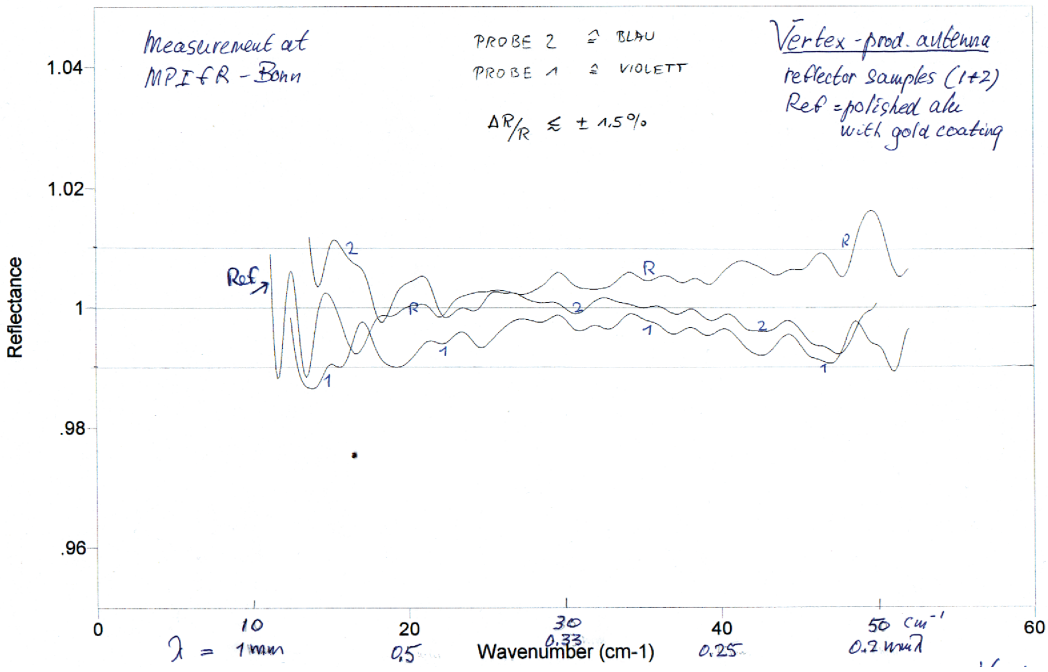


Fig.1. Reflectivity of two samples of final Vertex reflector (1, 2) and the reference (R). The wiggles are caused by small instabilities in the equipment.

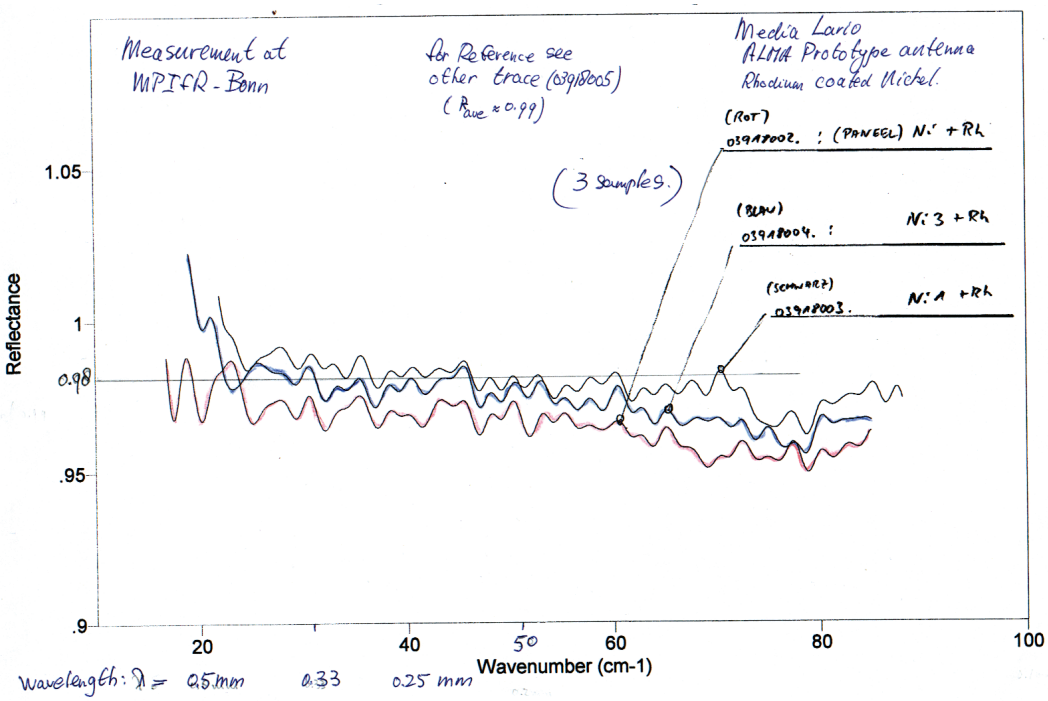


Fig.2a. Reflectivity of three samples of the AEC prototype reflector. The reference (shown below) also slowly decreases with increasing frequency. This, and the small wiggles are due to the measuring equipment. The AEM production antennas employ the same surface finish.

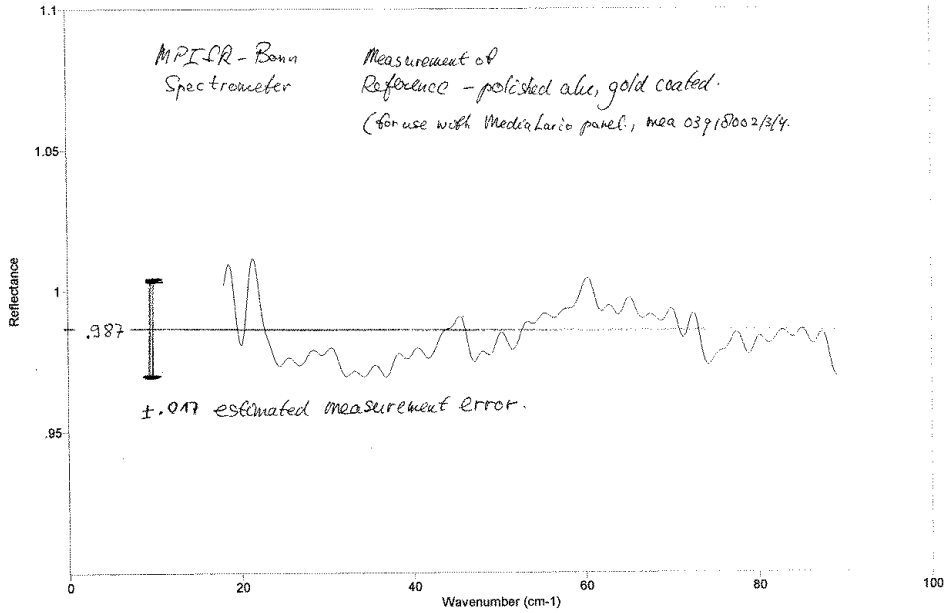


Fig. 2b. The spectrum of the reference disk (gold) during the measurements of Fig.2a. The measurement uncertainty is about 1-2 percent.

Vertex made many experiments in finding the best solution. In Fig.3. we show the reflectivity of some samples which did not perform satisfactorily. These surfaces were etched with a poor result (#2), chromatized (#3) or anodized (#4). They are not acceptable for ALMA's purpose. These samples were not studied further and these results are not included in Table 2.

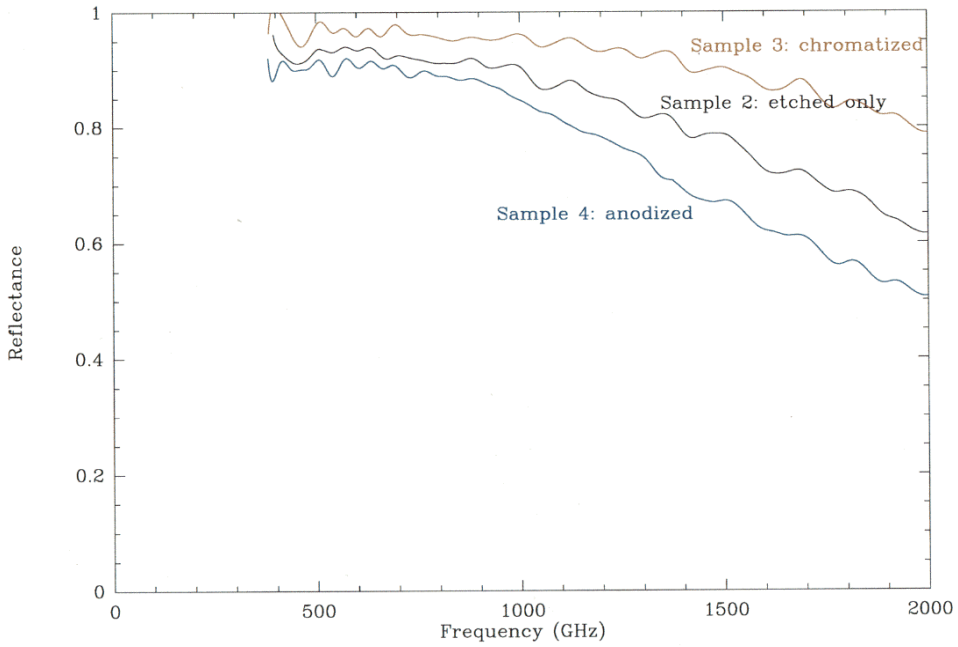


Fig.3. Reflectivity of samples with different surface finish. These were not considered acceptable and were not studied for other characteristics.

### 4. Measurement of scattering distribution at visible light (Buzzoni)

These measurements were performed in the optics laboratory of ESO in Garching.

#### 4.1. Measurement set-up.

A quartz tungsten halogen lamp illuminates the sample. The detector is a silicon photodiode with a spectral response range: 300-1000nm and peak sensitivity at 700nm.

The sample is placed perpendicular to the illuminating beam and we scan the detector to measure the scattered flux. We have an over/under angle of 4 degrees between the incident beam and the detector axis. This is to avoid shadowing of the detector onto the sample. This means that the sample is tilted by 2 degrees in a plane perpendicular to the scan plane

Schematic drawing of the set-up for measuring the scattering angle.

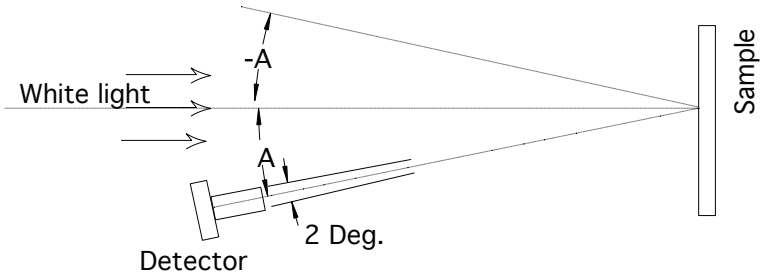


#### 4.2. Measurements and results.

The detector was scanned between –90 to 90 degrees by a 1 degree-step. An aluminised glass mirror was scanned to show the angular resolution of the set-up.

The samples with a surface of a fine groove structure diffract the light in one direction like a diffraction grating. For that reason we scanned the samples in the diffracting direction and perpendicular to that direction, called x- and y-direction. We note that the scanning in only two directions does not provide full information on the angular distribution of the scattered radiation. This is particularly the case for the Forcier samples, because the spatial distribution of the grooves does not show a strong symmetry. On the other hand the grooving of the Vertex samples was more regular over the sample, (it gives a “bull’s eye” impression) and the scattering distribution is close to a ring at the expected angle from the normal (see results below). Although not shown here, this was confirmed qualitatively by projecting the scattered light onto a screen. A clear annulus of light was observed.

The results of the measurements are presented in Figures 4-9. The sandblasted samples invariably show an essentially isotropic distribution of scattered light over the entire measurement range of 180 degrees. For that reason, we have not reproduced all the figures for these cases here.

We first show the scattering pattern of the final choice for the ALMA reflector surface finish for the Vertex antenna (Fig.4). Essentially identical solutions are being applied to the production antennas of the array. These surfaces scatter the visual radiation over a wide angle and exhibit on axis only 1-2 percent intensity of the infalling radiation.

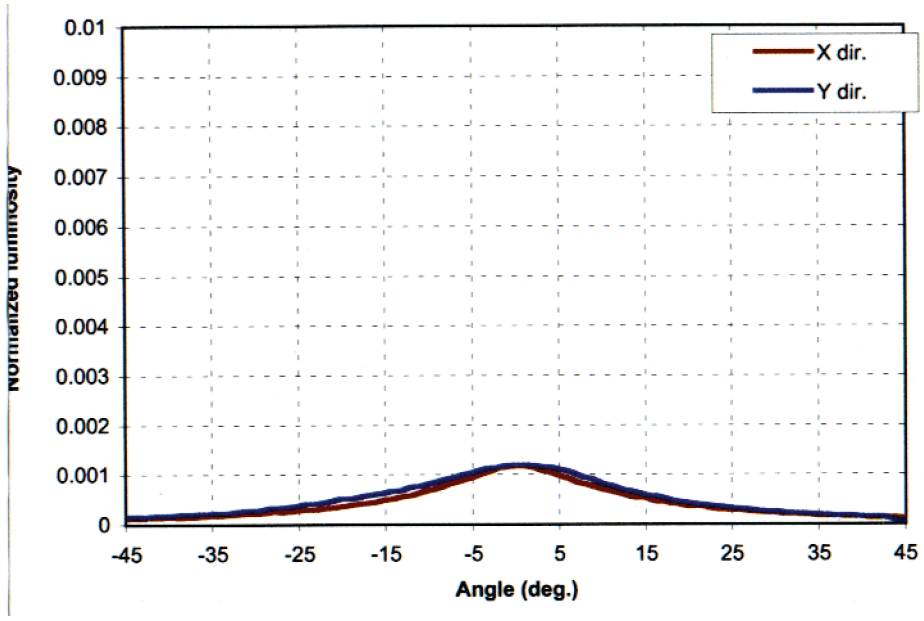


Fig.4. Scattering pattern of the final reflector choice for the Vertex prototype ALMA antenna. The production antennas employ identical surfaces. Measurements in two orthogonal planes show essentially identical results.

A completely different situation is illustrated in Figure 5, which shows the scattering from a machined sample with grooves. Here the grating effect is clearly visible with maxima in the grating ring of 13 percent of the incident power.

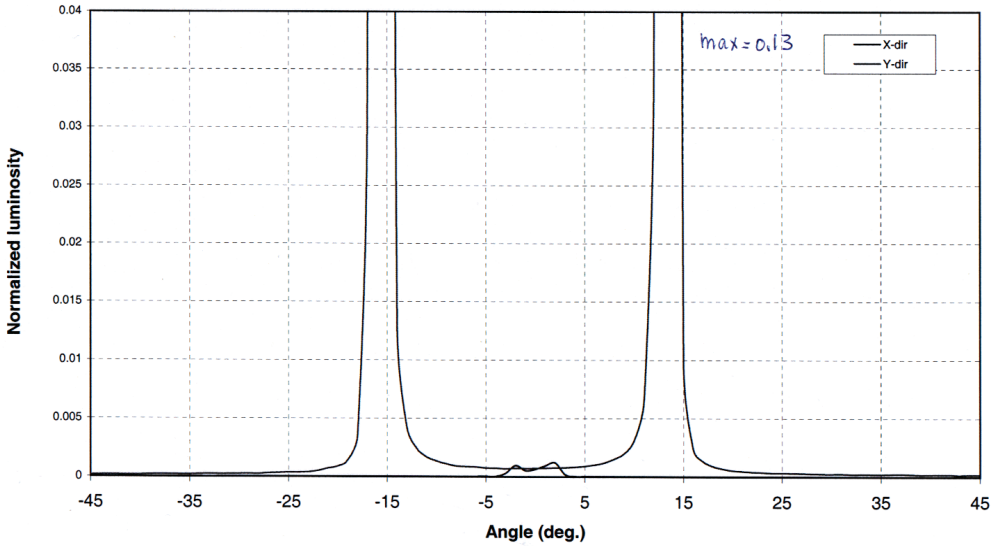


Fig. 5. Scattering pattern of the Vertex sample Nr.1 with a grooved machining pattern, showing the strong "grating" at about 15 degrees from the normal with a maximum of 13 percent of specular reflection from a flat plate. Such "sidelobes" could cause significant temperature rises on the antenna structure, for instance the quadripod. Note the very low scattering in the perpendicular direction between –5 and +5 degrees.

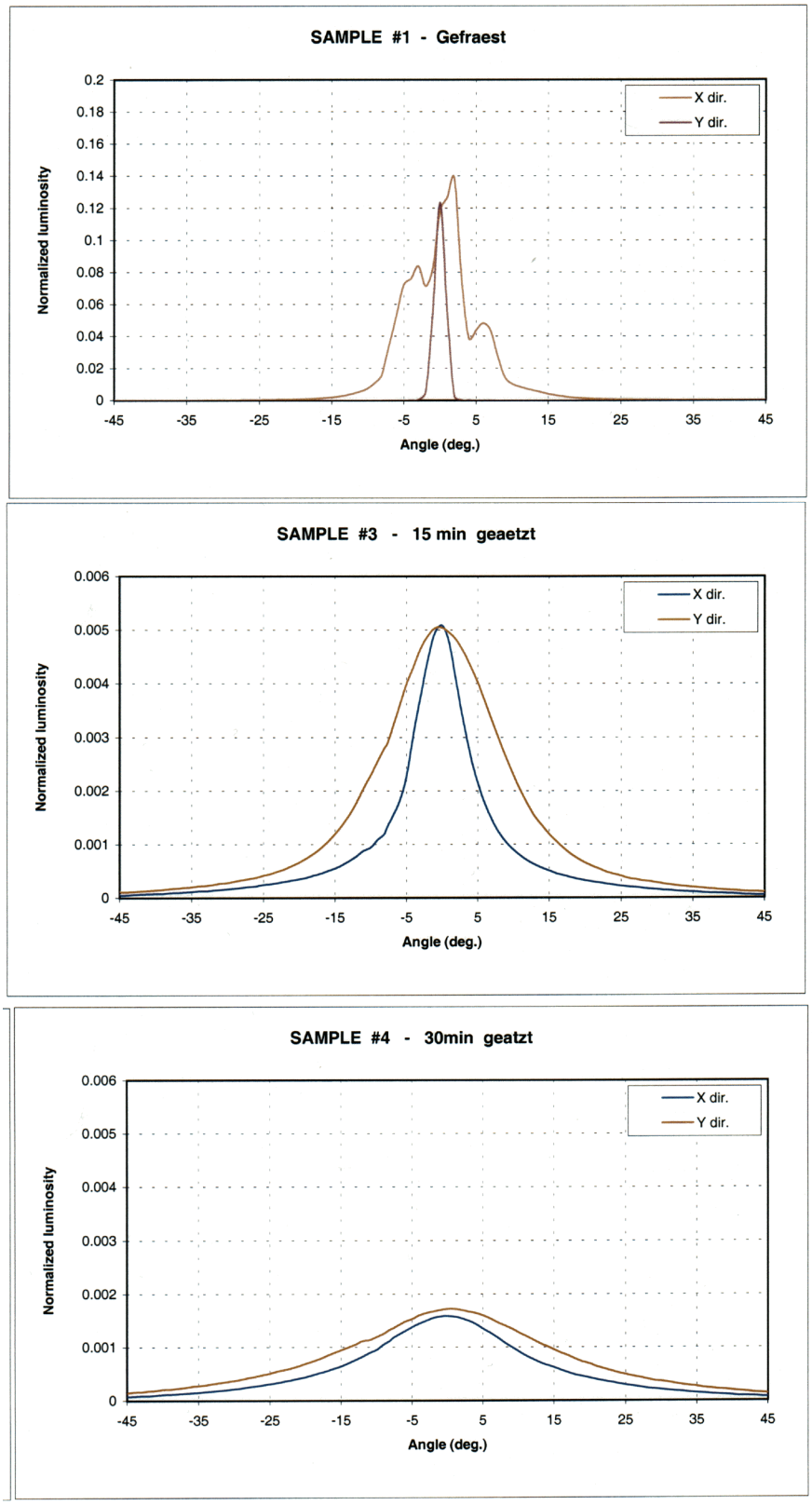


Fig. 6. Vertex first trials with etching. The machined sample (top) shows significant reflectivity in a narrow angular range. The etched curves are broad and have a low maximum.

When the sandblasting of the machined panels showed to have an undesirable influence on the overall shape of the thin panel surface, Vertex turned to etching techniques to "dull" the shiny reflector surface. An example of such a technique is shown in Fig.6.

The top frame shows the scattering pattern of the sample as it emerges form the machining process ("gefraest"). It reaches about 13 percent reflectivity and the scattering is confined to a rather narrow angular region. The structure in the x-direction is undoubtedly due by the machining pattern of the cutting head. Such machined samples were then chemically etched ("geetzt") for 15 and 30 minutes, respectively, with the results shown in the lower two frames. After 30 minutes etching the intensity in the specular direction has been lowered to about 3 percent, and the scattering is shows a broad featureless structure over a large angular region. This result was considered acceptable and the final ALMA panels are treated in this way to achieve a similar scattering behaviour, as shown in Fig. 4. Details of the etching process are proprietary and have not been published.

As noted, the Media Lario panels for the AEC antenna have a skin of nickel, chemically deposited onto a steel mandrel, which has been machined in the correct curvature. During the replication procedure the fine structure in the mandrel's surface is transferred to the surface of the nickel skin. A number of different surface treatments of the mandrel were tried to obtain a panel surface which scatters the visual light effectively. This procedure was successful, as shown in Figs. 7 and 8. In Fig.7 we show the scattering curve of the final panel choice for the prototype antenna. An essentially identical solution is used for the 25 production antennas. The nickel surface does not show the required thermo-optical behaviour; its absorptance is too high leading to an undesirably high temperature of the panel during solar observations. This has been ameliorated by coating the nickel surface with 200 nm rhodium. The coating does not have a noticeable effect on the scattering behaviour as shown in the two right hand frames of Fig.8. The upper curve is for sandblasted nickel, as released from the mandrel, the lower frame shows the result of a similar sample coated with a few hundred nanometers of aluminium.

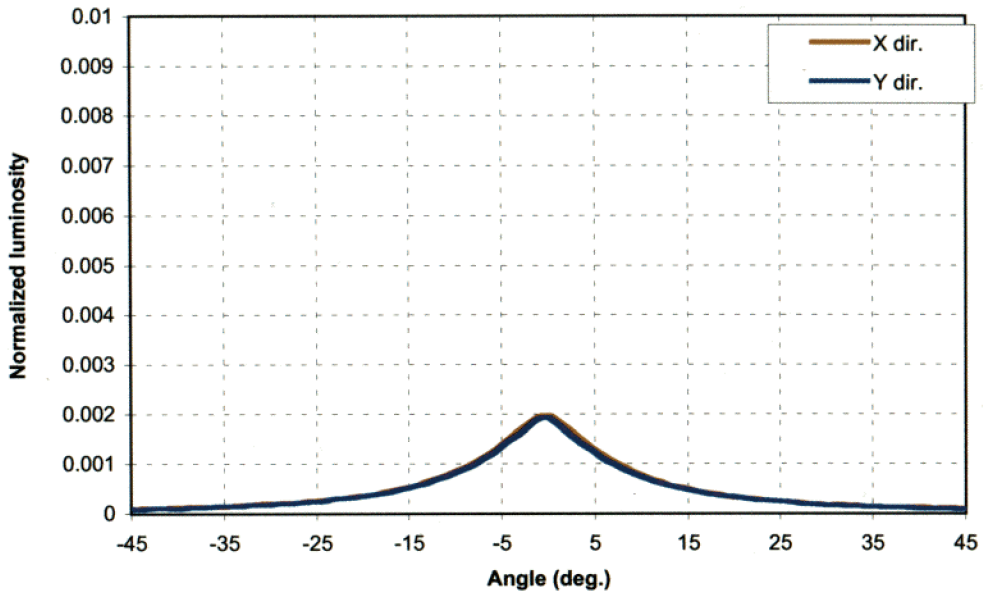


Fig.7. Scattering pattern of the final reflector choice for the AEC prototype ALMA antenna. The production antennas employ identical surfaces. Measurements in two orthogonal planes show essentially identical results.

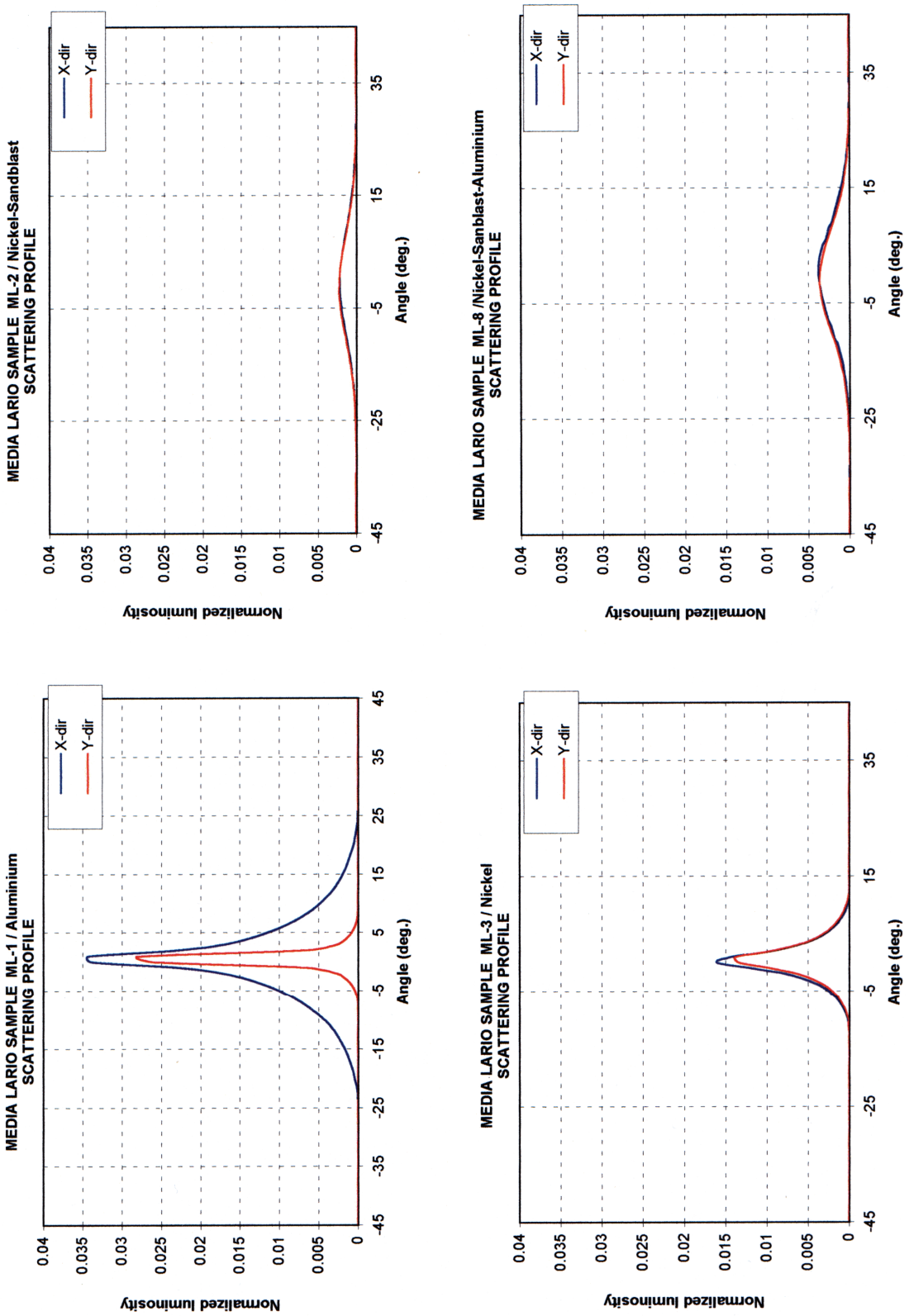


Fig. 8. Scattering patterns of some of the Media Lario samples. The sandblasted samples (right) show very low and broad scattering levels. The aluminium and nickel surfaces have a sharper scattering profile, but at a low and acceptable level of a few percent.

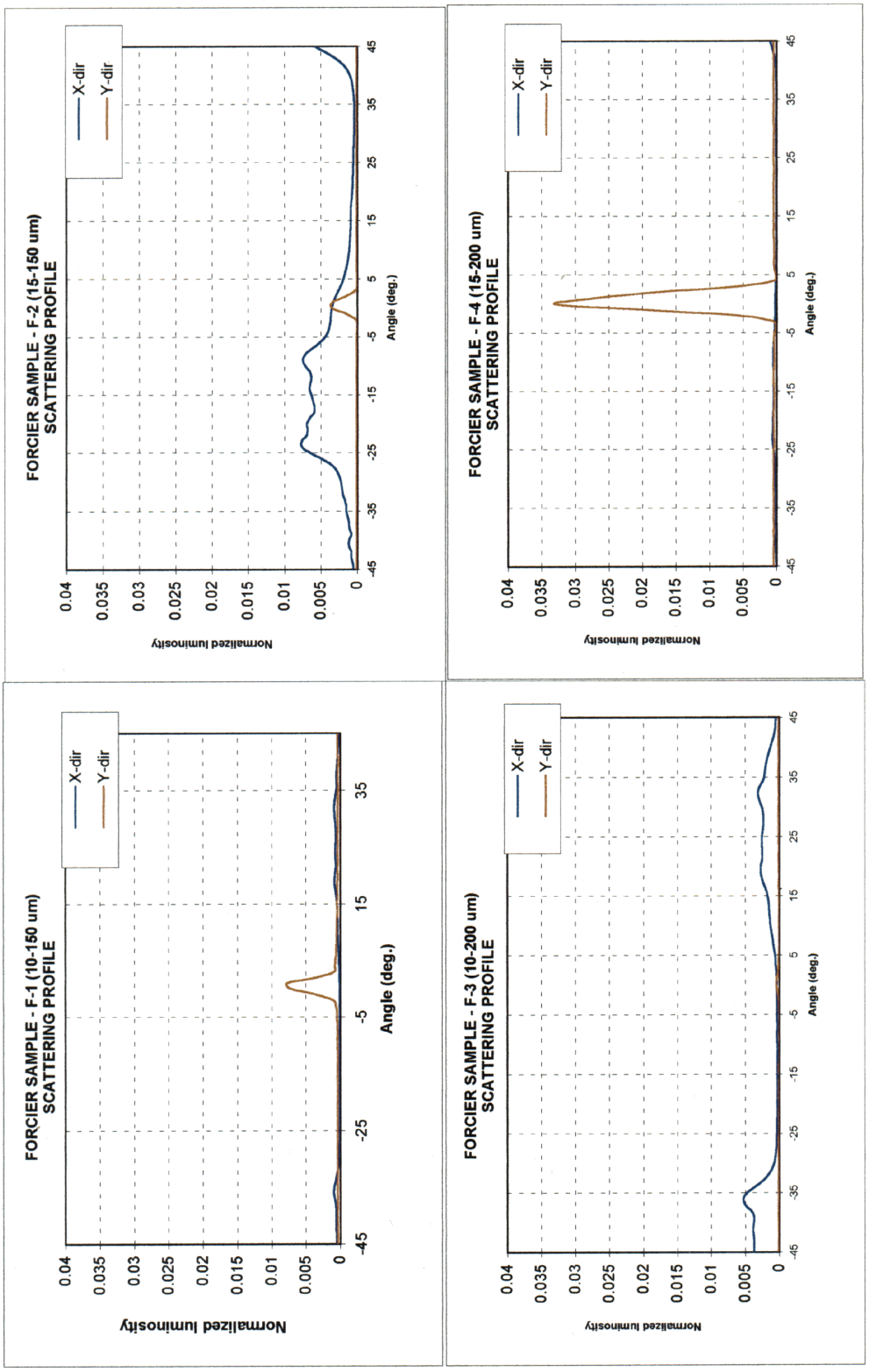


Fig. 9. Scattering patterns of the Forcier samples. The very irregular machining pattern causes very broad and essentially unstructured scattering in both perpendicular planes of measurement. Even the rather sharp feature at right bottom reaches only 3 percent.

Finally, in Fig. 9 we show the scattering patterns of the Forcier samples. The highly irregular machining pattern of the cutting head causes a very effective low level scattering over a wide angular region. In terms of scattering solar light this procedure is the most effective.

### 4.3. Specular reflectance.

The specular reflectance was measured at near normal incidence at 633nm. The detector acceptance angle is 2 degrees. The reflectance of the aluminium reference mirror was measured to be 0.86. The measured values are given in the column "visual specular reflectance "of Table 2.

Set-up:

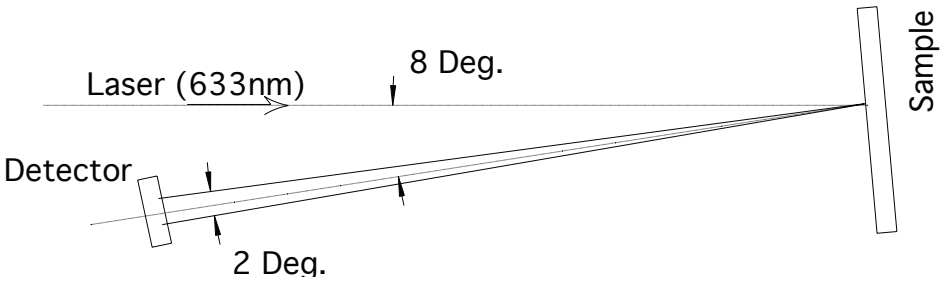


It is obvious that both the grooving and sandblasting of the surface decrease the specular reflectance to very small values, normally less than one percent. There appears to be no significant difference between the two methods of surface treatment in this respect. The electroformed, untreated "clear" samples of Nickel and Aluminium show a reflectance a factor 3 and 10 higher, respectively, than the sandblasted samples. Note that these samples, being replicated from a mold, do not provide a clear reflection when viewed in visible light. Thus the reflectance is still much below that of an "optical" mirror.

The sandblasted Vertex samples (being received after these reflectance measurements were done) were not measured this way. Their scattering pattern was measured however, as shown in the Figures.

## 5. Measurement of thermo-optical properties in the visible-infrared (Polsak)

These measurements were performed in the Materials and Processes Division of ESTEC in Noordwijk and reported in D-TOS/QMC Reports 2001/92 and 2001/120. Only a subset of the samples of Table 1 has been measured.

### 5.1 Measurement of solar reflection coefficients

Initially, the reflectivity spectra of the sample were measured using the Cary-5 UV-VIS-NIR photo-spectrometer fitted with an integrating reflectance sphere. Then the solar reflection coefficient was calculated by integrating the sample reflectivity spectra over the solar energy

spectrum (given by ASTM E490-73a) in the critical wavelength range of 250 nm to 2500 nm. Dividing the results of this integration by the total solar energy indicated the fraction of reflected solar energy ($R_S$), subtracting this value from 1 resulted in the solar absorption coefficient ($\alpha_S$).

### 5.2 Measurement of normal Infrared reflectivity

Measurements of sample surface normal infra-red reflectivity ($R_{n\text{-}IR}$) were performed by using a Gier-Dunkle DB100 infra-red reflectometer. This device directly measured the infra-red radiation reflected from a sample surface that originated from a thermal source within the test unit. The reflectivity measurements were relative to the standard reference reflectance of two calibration sample surfaces, which were traceable to a reference source held at Gier-Dunkle Instruments INC, CA, USA.

From Kirchhoff's radiation laws, the infra-red emissivity of a material is equal to its infra-red absorption when maintained at the same temperature. In addition, for non-transparent materials the IR reflectivity indicates the radiation that is not absorbed into the material. Therefore, subtraction of the reflectivity from 1 will equal the absorption, and hence, the emissivity of the material. From these principles the measured normal infra-red reflectivity ($R_{n\text{-}IR}$) can be used to calculate the normal infra-red emissivity ($\varepsilon_{n\text{-}IR}$).

### 5.3. Results

The results are collected in Table 2 in the columns "solar absorptance" and "IR normal emittance". The thermo-optical properties are strongly dependent on the roughness of the sample surface and less on the bulk material of the sample. The sandblasted aluminium and uncoated nickel samples show a high value for the absorptance (0.45), while the machined surfaces have a much lower values of about 0.13. A similar low values is obtained by coating the nickel panel with aluminium or rhodium. The IR emittance of the sandblasted aluminium (0.25) is 4-5 times higher than that of machined aluminium or the electroformed nickel (0.06).

## 6. Discussion (Baars)

In this Report we have summarised the results of a comprehensive program of measurements of all important parameters of materials, possibly suitable for reflector panels of a submillimeter wavelength radio telescope operating in the open air at a high and arid site. The following characteristics were measured:

1. reflectivity at near normal incidence over the frequency range 250 – 1500 GHz (wavelength 0.2 – 1.2 mm). This is the primary parameter which determines the suitability of the material and its surface treatment for the efficient observation of submillimeter radiation from astronomical sources.
2. solar absorptance and near-IR emittance. This quantity is of importance for the expected changes in temperature of the reflector between day time under solar heating and night time, when the reflector radiates towards the cold sky. We are particularly concerned with the temperature gradient through the panel, which causes deformation and hence a deterioration of the efficiency of the reflector at short submillimeter wavelengths.
3. Scattering of solar radiation over a large solid angle. Here we are concerned with the level of specular reflection of a highly smooth surface and the risk of unacceptably high heat loading of the subreflector and the receiver systems during solar observations. It is required that the reflector scatters visible light nearly isotropically over a large solid angle.

Although the primary radio wavelength is still larger than the visible/IR by a factor of several hundred, the three characteristics above are partially mutually inconsistent. The measurements reported here enable us to choose a material and surface finishing to provide the best compromise for our application.

The material of choice for most radio telescope reflectors is aluminium. Rolled or machined aluminium exhibits excellent reflectivity to frequencies well above one THz. If the surface is smooth and shiny (polished), the reflective loss is of the order of one percent. Our measurements indicate also excellent reflectivity near one for nickel, the material of the electroformed Media Lario panels. Thus nickel is an acceptable reflector material for submm telescopes.

Clearly, smooth and particularly polished aluminium will provide significant specular reflection of visible light. To minimise this (point 3 above), some samples have been machined with grooves to spread the radiation away form the specular direction. The measurements show that the detailed geometry of this grooving determines strongly the shape of the scatter pattern. The highly regular grooves of the Vertex samples indeed scatter the radiation very effectively away form the specular direction, but the resulting annular scattering lobe is quite narrow and rather intense. The surface acts like a grating. This could cause problems, if the observed source is several degrees away from the direction to the Sun (which will happen often in planetary observations) and the scatter lobe strikes the subreflector or the quadripod. This effect is much less pronounced with the Forcier samples, where the grooving is spatially very irregular and consequently the scattering solid angle is larger and without a clear shape.

The grooving of typical size 10-20 $\mu$m deep and 100-200 $\mu$m wide also causes a visible decline in the submm reflectivity whenever the wavelength is of the order of the groove spacing. This is probably due to the apearance of grating lobes (see Fig. 5). Thus, while the results are still acceptable for the frequency range of ALMA (< 1 THz), such panels will show a noticeable decrease in efficiency at higher frequencies. These frequencies are not impossible to observe from Chajnantor and particularly the smaller ACA antennas should be able to perform observations in the 1 – 1.5 THz region. The Forcier samples exhibit a slightly larger reflection loss (about two percent) than the other aluminium samples (typically one percent). We are not certain that this difference is real, because it is within the measurement error of the instrument, as mentioned in Section 3.

Considering the obvious disadvantages of the grooving procedure (which in most cases involves also an increased fabrication cost), other means of effectively scattering solar light have been considered. Sandblasting the panel surface was considered a viable solution, provided the action would not cause permanent deformation in the panel superseding the allowable small error tolerance. Vertex provided samples of sandblasted aluminium and Media Lario furnished sandblasted samples of nickel, some of them coated with a thin aluminium layer after sandblasting. In the Media Lario technique of evaporation onto a mold, the obvious way is to sandblast the mold. This has the great advantage that the resulting panel will not be subjected to the pressures of the blasting process.

All sandblasted samples showed an essentially isotropic scattering of visible light over a very large solid angle, approaching $2\pi$ steradians in most cases. This surface finish seems to be ideal for avoidance of "hot spots" when observing the Sun or its neighbourhood. It should be noted that the electroforming technique leads to an optically "dull" appearance of the surface, which in itself scatters light more effectively than a machined aluminium surface.

The submm reflectivity of the sandblasted samples appears to be a trifle smaller than that of the machined specimens; again the measured difference of 1-2 percent is not significant in view of

the measurement accuracy. Thus it appears that the sandblasting provides a solution which satisfies both the rf reflectivity and the solar scattering requirements.

However, the question now arises whether the changes in the fine structure of the surface material, caused by the sandblasting process, could have an adverse effect on the optical/near IR absorption and emission coefficients. An increase in this parameter could lead to excessive heating of the panel under solar illumination and strong cooling at night towards the cold sky. Both effects would lead to an increase of the temperature gradient through the reflector panel, causing additional deformation of the panel. These quantities were measured, as reported in Section 5.

Indeed, we see a significant increase in absorptance/emittance values for the sandblasted samples compared to the regularly grooved Vertex specimens. Remarkably, the Forcier grooved samples show values between those of the wider grooved and sandblasted samples. The very fine grooving of the Forcier reflector appears to increase the absorptance.

The electroformed Media Lario samples, be they clear or sandblasted, have a high value of the absorptance, while the emittance remains low. Supposedly this is a result of the evaporation procedure. Interestingly, the sandblasted Media Lario sample which received a thin aluminium coating after sandblasting is much better and shows an absorptance as measured on pure aluminium. An alternative experiment was made with a coating of rhodium. Here too, acceptable low values of the absorptance and emittance were found (Table 2), comparable to those of aluminium. Because rhodium exhibits a better protection against environmental influences, the final decision of Media Lario was to coat the ML panels with 200 nm of rhodium, despite the fact that the submillimeter reflectivity of rhodium is slightly less than of aluminium (Table2).

Vertex experienced problems of panel shape stability under sandblasting and experimented with other surface treatments, like anodizing procedures, and chemical etching. Their final solution was to chemically etch the panels, leading to acceptable values for all parameters, as shown in Table 2. The VM-final entry in Table 2 did not have its absorptance and emittance measured in this program, but the procedure is similar to that of VM4, where acceptable values of these quantities were measured.

We conclude with mentioning some highly accurate measurements of the rf-reflectivity of several of these samples in the frequency range from 100-200 GHz. These were made with a Fabry-Perot resonator at the Applied Physics Institute of the Russian Academy of Sciences in Nizhny Novgorad in a joint effort of that Institute, and ESA. Results have been published by Parshin et al. (2002) and Myasnikova et al. (2006). The accuracy of these measurements of the reflectiviy is of the order of one permille. At 200 GHz the reflective loss of pure aluminium is measured to be 0.25%, of nickel 0.35% and of rhodium 0.35% also. Unfortunately there is no overlap in the frequency coverage between these measurements and those made at MPIfR, which start at 250 GHz. But it is safe to say that the difference is small enough to confirm that the values “1.00” given in Table 2 at 300 GHz are correct to a few tenths of a percent. Because the relative accuracy of the MPIfR measurements over the frequency range is better than one percent, the values at the higher frequencies in Table 2 can be considered trustworthy.

*Acknowledgement.*

The main author of this report and instigator of the measurement program wants to record his thanks to ESO, MPIfR and ESA for making their facilities and personnel available for these measurements. He also wants to thank his co-authors for their efforts and contributions, which often could only be performed by interrupting their regular work.

References

V.V. Parshin, S.E. Myasnikova, G. Valsecchi, K. van ‘t Klooster, “Reflectivity investigations of metal samples in the frequency range 110-200 GHz”, 25th Antenna Workshop on “Satellite Antenna Technology”, ESTEC, 2002, pp. 689-696.

S.E. Myasnikova , V.V. Parshin, K. van ‘t Klooster, G. Valsecchi, “Reflectivity of antenna and mirrors reflectors ar 110 and 200 GHz”, ???, 2006

| Origin | Code | Maerial | Surface finish | Detail | RF<br><br>300 | Reflectance<br><br>600 | (GHz)<br><br>1000 | Visual specular reflectance | Solar absorptance | IR normal emittance | Figures |
|---|---|---|---|---|---|---|---|---|---|---|---|
| Vertex | V1 | Alumin. | Grooves | 250 $\mu$m, 3° | 0.99 | 1.0 | 0.99 | 0.0022 | 0.188 | 0.04 | 5 |
| | V2 | Alu | Grooves | 250 $\mu$m, 6° | 0.99 | 0.99 | 0.99 | | 0.080 | 0.03 | |
| | VS1 | Alu | Sandblasted | 1 bar, long | 0.98 | 0.98 | 0.98 | | 0.483 | 0.24 | |
| | VS2 | Alu | Sand.-polished | 1 bar, long | 0.98 | 0.98 | 0.98 | | 0.313 | 0.13 | |
| | VS3 | Alu | Sandblasted | 2 bar, short | 0.98 | 0.98 | 0.98 | | 0.568 | 0.30 | |
| | VM1 | Alu | Fine-machined | pure | 1.0 | 1.0 | 1.0 | 0.12 | 0.157 | 0.04 | 6 |
| | VM2 | Alu | Machined | painted | 0.98 | 0.5 | 0.5 | 0.0005 | 0.449 | 0.52 | resonance |
| | VM3 | Alu | Macined | Etched 15 min. | 1.0 | 0.99 | 0.99 | 0.005 | 0.125 | 0.06 | 6 |
| | VM4 | Alu | Machined | Etched 30 min. | 1.0 | 0.99 | 0.98 | 0.0014 | 0.125 | 0.08 | 6 |
| | VM5 | Alu | Machined | Laser annealed | 0.99 | 0.98 | 0.97 | | | | |
| | VM-final | Alu | Machined | Chem. etched | 1.0 | 0.995 | 0.99 | 0.025 | | | 1, 4 |
| Forcier | F1 | Alu | Fine grooves | 150 $\mu$m pitch, 10 $\mu$m deep | 0.99 | 0.98 | 0.98 | 0.0015 | | | 9 |
| | F2 | Alu | Fine grooves | 150, 15 $\mu$m | 0.99 | 0.98 | 0.97 | 0.006 | 0.192 | 0.10 | 9 |
| | F3 | Alu | fine grooves | 200, 10 $\mu$m | 0.98 | 0.98 | 0.98 | 0.0008 | 0.287 | 0.09 | 9 |
| | F4 | Alu | Fine grooves | 200, 15 $\mu$m | 0.98 | 0.98 | 0.98 | 0.0058 | | | 9 |
| Media Lario | ML1, 7 | Alu | Clear | | 1.0 | 1.0 | 1.0 | 0.031, 0.045 | 0.410 | 0.04 | 8 |
| | ML2, 4, 9 | Nickel | Sandblasted | | 0.99 | 0.99 | 0.99 | 0.0021 | 0.451 | 0.06 | 8 |
| | ML3 | Nickel | Clear | | 1.0 | 1.0 | 0.99 | 0.009 | 0.451 | 0.06 | 8 |
| | ML5, 6, 8 | Nickel | Sandblasted | Alu coating | 1.0 | 1.0 | 1.0 | 0.0036 | 0.158 | 0.06 | 8 |
| | ML10 | Nickel | polished | | 1.0 | 0.99 | 0.99 | 0.0094 | 0.449 | 0.05 | |
| | ML-final | Nickel | Rhodium coat | 200 $\mu$m | 1.0 | 0.99 | 0.99 | | 0.18 | 0.03 | 2, 7 |

**Table 2. Summary of characteristics and measurement results on ALMA antenna reflector samples.**